Soft X-ray Microscopy at the NSLS

TOBIAS BEETZ,[1] MICHAEL FESER,[1] HOLGER FLECKENSTEIN,[1]
BENJAMIN HORNBERGER,[1] CHRIS JACOBSEN,[1] JANOS KIRZ,[1] MIRNA LEROTIC,[1]
ENJU LIMA,[1] MING LU,[1] DAVID SAYRE,[1] DAVID SHAPIRO,[1] AARON STEIN,[2]
DON TENNANT,[3] AND SUE WIRICK[1]

[1]*Department of Physics & Astronomy, Stony Brook University, Stony Brook NY 11794, USA*
[2]*Brookhaven National Laboratory, Upton, NY 11973-5000, USA*
[3]*New Jersey Nanotechnology Consortium, 600–700 Mountain Ave, Murray Hill, NJ 07974, USA*

Soft X-ray microscopy has a long history at the National Synchrotron Light Source. Following earlier experiments with laboratory sources and at the Stanford Synchrotron Radiation Project [1], Janos Kirz, Harvey Rarback, and John Kenny of Stony Brook built a zone-plate-based scanning transmission X-ray microscope (STXM) at beamline U15 on the 750 MeV VUV ring that started operation in 1983 [2]; Malcolm Howells and collaborators started experiments in X-ray holography [3]; and David Sayre and collaborators started experiments in diffraction-based imaging [4,5]. Harald Ade and collaborators developed the first scanning photoemission microscope using zone plate optics that was subsequently upgraded [6], though this instrument is no longer in operation. One can trace through the developments of successive STXMs at the NSLS X-ray ring: STXM II at a prototype and then a dedicated microscopy beamline [7]; STXM III with improved spatial resolution [8]; and the present instrument, STXM IV, which will be described later. These activities have relied on the development of high-resolution zone plate optics by e-beam lithography at IBM [9], Berkeley [10], and more recently Stony Brook and Bell Labs [11]. Holography activities have also continued, evolving to ~50 nm resolution experiments with photoresists in the in-line geometry [12] and zone plates in the Fourier transform geometry [13]. Applications have included the mapping of calcium in bone [14,15], the imaging of cellular and subcellular structures and studies of radiation damage limitations in biology [16], and the pioneering of absorption spectromicroscopy for studies of polymers [17,18] and biomedical specimens [15,19]. A considerable effort has gone into the development of new methods and imaging modalities, including tomography [20,21], darkfield imaging [22], Wigner phase contrast [23] and Nomarski differential interference contrast [24], and luminescence [25]. Spectromicroscopy studies have been complemented by spectroscopy studies of synthetic polymers and bioorganic molecules [26], and of radiation damage processes [27]. It is exciting to see the contributions of many scientists in these past activities, as well as ongoing activities and new efforts that we describe here.

STXM IV microscope:
Spectromicroscopy and phase contrast

About 15 years ago, a 35 period hybrid undulator was installed on the 2.8 GeV NSLS X-ray ring for soft X-ray experiments. The initial soft X-ray microscopy undulator beamline was upgraded in 1996 to provide independent monochromators for two end stations with higher throughput and energy resolution and better control of spatial coherence [28]. More recently, two copies of a newly designed microscope (STXM IV) have been installed that provide new capabilities, including more stable optical alignment and higher resolution capabilities, and the ability to scan either of two detectors at micrometer precision [29]. These capabilities have been exploited by installing a segmented silicon detector that can be used to deliver both amplitude and phase contrast images by reconstruction of data acquired during a single scan [30] (see Figure 1). However, the primary applications of these microscopes have been for spectromicroscopy, where several images and/or point spectra are taken at absorption edges to deliver chemical information based on near-edge absorption structure (XANES or NEXAFS) [17,31]. More recently, a mode of imaging has been developed whereby a sequence of images is automatically acquired and aligned, yielding a "stack" of data in position and photon energy (x,y,E) [32]. Alignment based on image features will become unnecessary in the future, as an upgrade to STXM V is underway whereby a laser interferometer will be used to provide closed-feedback-loop position information while scanning not row-by-row but continuously over the whole specimen so as to essentially eliminate computer overhead time.

In the case of specimens that can be treated as involving a mixture of a limited number of spectroscopically distinct materials with known spectra, compositional maps can be obtained using singular value decomposition fitting [19,33]. However, the assumption that all spectral signatures are known in advance does not always apply, especially in biology and environmental science. For these specimens, we have turned to multivariate statistical analysis methods. Principal component analy-

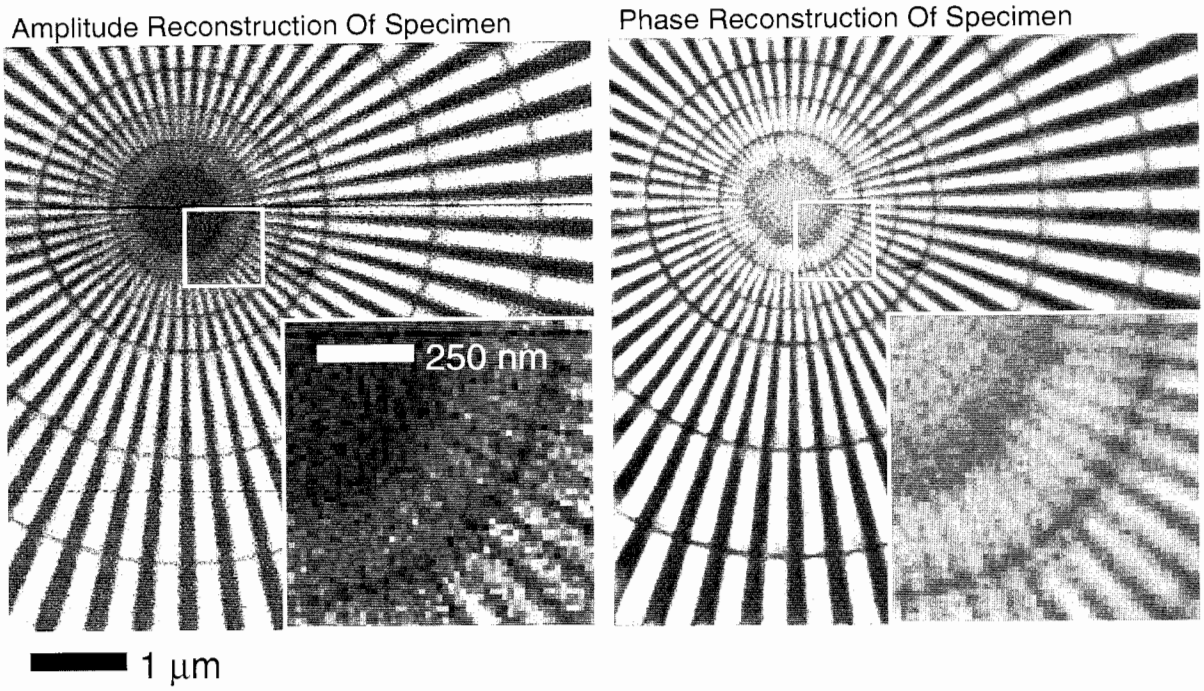

Figure 1: Phase gradients and periodicities in the specimen alter the distribution of energy in the detector plane in a scanning transmission X-ray microscope. Feser et al. have used a segmented Si detector to record this redistribution and to obtain both amplitude and phase contrast images from a single scan of the specimen. Shown here are the amplitude (left) and phase (right) reconstructions of a microfabricated test pattern. The phase contrast image has less noise due to normalizing out source intensity fluctuations, and a phase that is in good agreement with the value expected for 100 nm thick Ge at 520 eV [30].

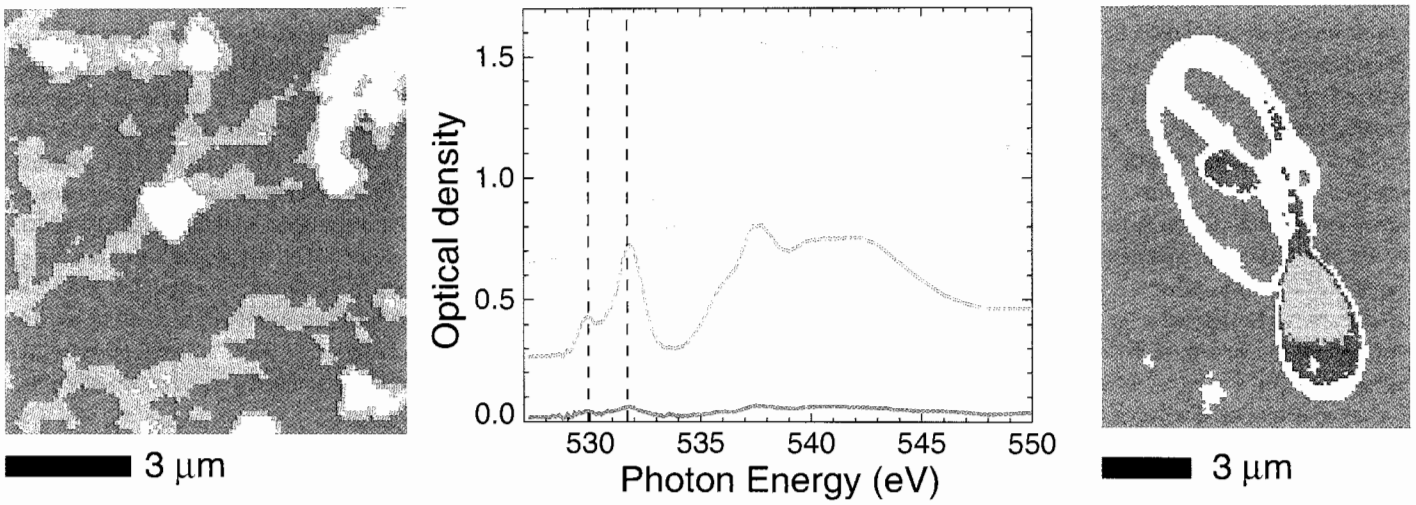

Figure 2: Cluster analysis of spectromicroscopy data [35]. Shown at left and center are analyses results of ferrihydrite-haematite transformation products in the presence of lutetium investigated by Schäfer et al. as part of a study of the colloidal transport properties of radionuclides (lutetium is used as a homologue of americium). By cluster analysis of eigenspectra of a covariance matrix formed from all spectra over a 527 to 550 eV energy range, three spectroscopically distinct regions were identified. The blue region is a background region with little haematite present. The red regions have a spectrum with resonances at 529.9 and 537.1 eV characteristic of pure haematite. The green regions have a spectrum with reduced optical density at 529.9 eV, indicating that lutetium is incorporated into the haematite. At right is shown the cluster analysis image of an air-dried human sperm, indicating that cluster analysis provides spectroscopic sorting even when applied to biological specimens with complex spectra.

sis, or PCA, can be used to represent the set of spectra that exist in all pixels in terms of a linear combination of a limited set of eigenspectra; this provides insight into the number of spectroscopically distinguishable components that exist in the specimen, and the spatial regions and photon energies where most of the variations in composition are located [34]. In fact, PCA serves to both orthogonalize (into the linearly independent eigenspectra) and noise-filter (by reducing the data set from images at ~100 photon energies to images at typically 4–8 principal eigenspectra) the data; one can then use cluster analysis or pattern matching to group pixels according to commonality of their spectra and do target fitting to the spectra of compounds that are thought to exist in the specimen [35]. An example is shown in Figure 2.

A number of studies are being carried out using soft X-ray spectromicroscopy at the NSLS. The Stony Brook group (including Yefim Sheynkin) is studying morphology and biochemistry in sperm. Ongoing studies in geochemistry include measurements of the organic matter decay in the ocean by Jay Brandes (U. Texas) and collaborators; and in recent and ancient plant tissue by Kevin Boyce, George Cody, and collaborators [36] (see Figure 3). George Flynn and collaborators are studying the organic content of interplanetary dust particles and micrometeorites. Studies in environmental science include topics such as the phases of iron compounds that can take up radionuclides by Thorsten Schäfer, Jörg Rothe, and collaborators at INE Karlsruhe (see Figure 2); the degradation of organic matter at various soil depths by Marc Schumacher and collaborators at ETH Zurich; and the role of organics in altering uptake of metals by Maartin Nachtegaal, Donald Sparks, and collaborators at the University of Delaware. These and other projects rely on the capability of soft X-ray spectromicroscopy for nanoscale investigations of chemical heterogeneity.

An important consideration for many studies (especially those of wet organic specimens) is radiation damage. To minimize the effects of radiation damage, Jörg Maser led an effort to develop a cryo STXM for studying frozen hydrated specimens at liquid nitrogen temperatures, and showed that no mass loss could be observed at radiation doses as high as 10^{10} Gray, making it possible to obtain the first soft X-ray tomographic images of frozen hydrated mammalian cells [21,37]. However,

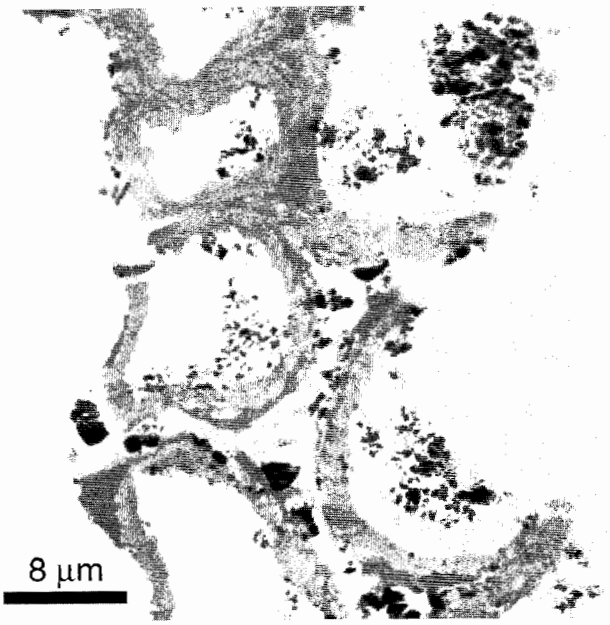

Figure 3: A cross section through a 45-million-year-old fossil of the wood Metasequoia milleri *imaged at 286.3 eV reveals preserved chemical differentiation related to the presence of lignin and polysaccharides within the wall of tracheid cells. From Boyce et al. [36].*

it has been somewhat surprising to see that the loss of near-edge absorption resonances in dry polymer films is *not* improved by operation at liquid nitrogen temperature [38]; further studies on this subject are planned after an upgrade of the cryo STXM to higher spatial resolution is completed.

Beyond direct zone plate imaging

Two projects are underway to explore imaging methods beyond direct zone plate imaging. Diffraction tomography is being developed to work with specimens that extend beyond the ~$4(dr_N)^2/\lambda$ depth of focus limit of incoherent imaging with a zone plate with outermost zone width of dr_N (about 0.7 micrometers at 2.3 nm with dr_N = 20 nm). This has involved the construction of an experimental apparatus [39] intended for rotation of frozen hydrated specimens through a ±80° tilt range, and the recording both of Fourier holograms using a zone-plate-generated point illumination source, and of Gabor holograms using a zone plate to magnify the hologram onto the CCD detector.

By recording the far-field diffraction pattern of a non-crystalline specimen, one has in principle information out to a maximum resolution as limited by the specimen rather than imposed by the optics (*4*). The trick is that one must properly phase this information so as to obtain an image. Using iterative algorithms [40], Miao, Sayre et al. demonstrated the recording and reconstruction of soft X-ray diffraction data [41]. New developments [42] with the same apparatus as above [39] include the recording of diffraction data from freeze-dried (see Figure 4) and frozen hydrated yeast cells, and studies of new phase retrieval algorithms [43]. Mentes et al. are also using this apparatus for reconstructions of magnetic structures from circular dichroism diffraction data [44].

Outlook

Brookhaven National Laboratory is establishing a new Center for Functional Nanomaterials, to be located next to the NSLS. This facility, to be completed in 2006, will provide access to the hard X-ray microprobes and soft X-ray microscopy beamlines at the NSLS, and will also provide capabilities in nanofabrication (including a JEOL JBX-9300FS electron beam lithography system) needed for the development of zone plate optics.

When the NSLS was designed in the late 1970s, the importance of high-brightness synchrotron radiation sources for coherent imaging experiments was beginning to be appreciated [45]; as a result, even though the NSLS is described as a second-generation machine, its brightness in the soft X-ray range is within about a factor of 20 of that of many third-generation machines. Nevertheless, the NSLS is now in advanced planning stages of a completely new facility (NSLS-II) that will involve a 3 GeV storage ring with 523 m diameter, 500 mA current, and a horizontal emittance of only 1 nm-radian so that it will deliver a time-averaged brightness of nearly 10^{21} photons/second/mm^2/mrad^2 in the soft X-ray range.

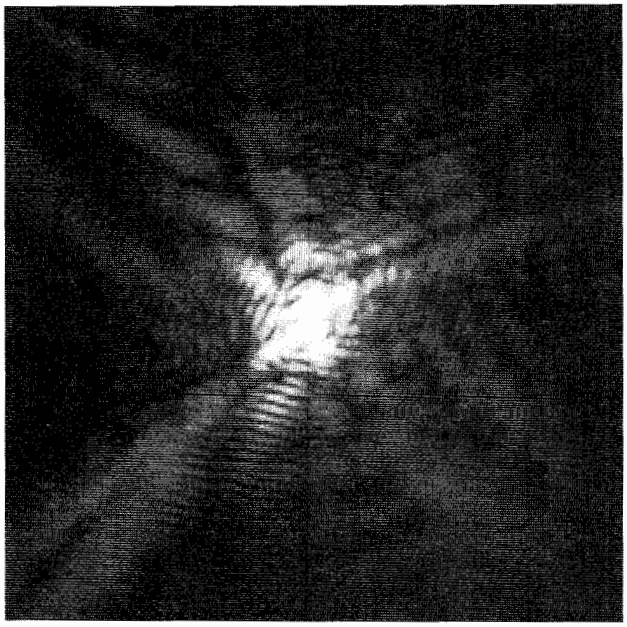

Figure 4: Soft X-ray diffraction pattern obtained by Shapiro et al. of an air-dried yeast cell recorded using 730 eV soft X-rays. The overall diffraction pattern at reduced exposure is shown. The inset is the pattern obtained with the CCD camera shifted to the corner and with increased exposure time, showing structure at 18 nm half-period. Present efforts are aimed at collecting diffraction data from freeze-dried and frozen hydrated specimens at a series of specimen orientations for 2D and 3D image reconstruction.

With new developments in microscopy methods, instrumentation, and applications, new optics to be developed within the Center for Functional Nanomaterials, and a new NSLS-II synchrotron radiation facility, the future for soft X-ray microscopy at Brookhaven National Laboratory looks bright indeed! ■

Acknowledgements

We thank our many colleagues and collaborators, including those not noted above. We thank the National Science Foundation for support under grants DBI-9986819, ECS-0099893, OCE-0221029, and CHE-0221934; the National Institutes of Health for support under grants EB00479-01A1 and GM64846-01; and the National Aeronautics and Space Administration for support under grant NAG5-12884. The National Synchrotron Light Source is supported by the U.S. Department of Energy, Division of Materials Sciences and Division of Chemical Sciences, under Contract No. DE-AC02-98CH10886.

References

1. H. Rarback et al, in *Scanned Image Microscopy,* E. A. Ash, ed. (London, 1980) pp. 449.
2. H. Rarback et al., in *X-ray Microscopy,* G. Schmahl, D. Rudolph, eds. (Springer-Verlag, Berlin, 1984), vol. 43, pp. 203.
3. M. R. Howells et al., in *Science with Soft X-rays,* F. J. Himpsel, R. W. Klaffky, eds. (Bellingham, Washington, 1984), vol. 447, pp. 193.
4. D. Sayre, in *Imaging Processes and Coherence in Physics,* M. Schlenker, ed. (Springer-Verlag, Berlin, 1980) pp. 229.
5. W. B. Yun et al., *Acta Crystallographica A* **43,** 131 (1987).
6. H. Ade et al., *Appl. Phys. Lett.* **56,** 1841 (1990); C.-H. Ko et al., *Rev. Sci. Inst.* **66,** 1416 (1995).
7. C. Buckley et al., *Rev. Sci. Inst.* **60,** 2444 (1989); H. Rarback et al., *J. X-ray Sci. Tech.* **2,** 274 (1990).
8. C. Jacobsen et al., *Opt. Comm.* **86,** 351 (1991).
9. D. Sayre, "Proposal for the utilization of electron beam technology in the fabrication of an image forming device for the soft X-ray region," *Tech. Report No. RC 3974 (#17965)* (IBM Research, 1972); D. Kern et al., in *Science with Soft X-rays,* F. J. Himpsel, R. W. Klaffky, eds. (SPIE, Upton, New York, 1984), vol. 447, pp. 204.
10. E. Anderson, D. Kern in X-ray Microscopy III, A. G. Michette, G. R. Morrison, and C. J. Buckley, eds. (Springer, Berlin, 1992), pp. 75–78.
11. S. Spector et al., *J. Vac. Sci. Tech. B* **15,** 2872 (1997); D. Tennant et al., in [46], p. 601; A. Stein et al., *J. Vac. Sci. Tech. B* **21,** 214 (2003).
12. M. Howells et al., *Science* **238,** 514 (1987); C. Jacobsen et al., *J. Opt. Soc. Am.* **A 7,** 1847 (1990); S. Lindaas et al., *J. Opt. Soc. Am.* **A 13,** 1788 (1996).
13. I. McNulty et al., *Science* **256,** 1009 (1992).
14. J. M. Kenney et al., *J. Micros.* **138,** 321 (1985).
15. C. Buckley et al., in *X-ray Microscopy and Spectromicroscopy,* J. Thieme et al., eds. (Berlin, 1998) pp. II.
16. J. R. Gilbert, J. Pine, in *Soft X-ray Microscopy,* C. Jacobsen, J. Trebes, eds. (SPIE, Bellingham, Washington, 1992), vol. 1741, pp. 402; S. Williams et al., *J. Micros.* **170,** 155 (1993); K. K. Goncz et al., *Cell Tiss. Res.* **280,** 519 (1995); P. M. Bennett et al., *J. Micros.* **172,** 109 (1993).
17. H. Ade et al., *Science* **258,** 972 (1992).
18. H. Ade, B. Hsiao, *Science* **262,** 1427 (1993); S. Zhu et al., *Nature* **400,** 49 (1999); A. P. Smith et al., *Appl. Spect.* **55,** 1676 (2001).
19. X. Zhang et al., *J. Struct. Bio.* **116,** 335 (1996).
20. W. S. Haddad et al., *Science* **266,** 1213 (1994).
21. Y. Wang et al., *J. Micros.* **197,** 80 (2000).
22. G. R. Morrison, M. T. Browne, *Rev. Sci. Inst.* **63,** 611 (1992); H. N. Chapman et al., *Ultramic.* **62,** 191 (1996); H. N. Chapman et al., *J. Micros. Soc. Am.* **2,** 53 (1996).
23. H. N. Chapman, *Ultramic.* **66,** 153 (1996).
24. F. Polack et al., in [46], p. 573.
25. C. Jacobsen et al., *J. Micros.* **172,** 121 (1993); M. M. Moronne, *Ultramic.* **77,** 23 (1999).
26. S. G. Urquhart et al., *J. Elect. Spect. Rel. Phenom.* **100,** 119 (1999); J. Boese et al., *J. Elect. Spect. Rel. Phenom.* **85,** 9 (1997); K. Kaznacheyev et al., *J. Phys. Chem. A* **106,** 3153 (2002).
27. X. Zhang et al., *J. Vac. Sci. Tech.* **B 13,** 1477 (1995); E. G. Rightor et al., *J. Phys. Chem.* **B 101,** 1950 (1997); T. Coffey et al., *J. Elect. Spect. Rel. Phenom.* **122,** 65 (2002).
28. B. Winn et al., *J. Synch. Rad.* **7,** 395 (2000).
29. M. Feser et al., in [46], p. 367; M. Feser et al., in *Soft X-ray and EUV imaging systems II,* D. A. Tichenor, J. A. Folta, eds. (SPIE, Bellingham, WA, 2001), vol. 4506, pp. 146.
30. M. Feser et al., in *X-ray micro- and nano-focusing: applications and techniques II,* I. McNulty, ed. (SPIE, Bellingham, WA, 2001), vol. 4499, pp. 117; M. Feser et al., *J. de Physique IV* **104,** 529 (2003).
31. X. Zhang et al., *Nucl. Inst. Meth. Phys. Res. B* **A 347,** 431 (1994).
32. C. Jacobsen et al., *J. Micros.* **197,** 173 (2000).
33. C. J. Buckley, in [46], p. 33.
34. P. L. King et al., *J. Vac. Sci. Tech.* **A 7,** 3301 (1989); A. Osanna, C. Jacobsen, in [46], p. 350.
35. C. Jacobsen et al., *J. de Physique IV* **104,** 623 (2003).
36. C. K. Boyce et al., *Geology* **30,** 1039 (2002).
37. J. Maser et al., J. Micros. **197,** 68 (2000).
38. T. Beetz, C. Jacobsen, *J. Synch. Rad.* **10,** 280–283 (2003).
39. T. Beetz et al., *J. de Physique IV* **104,** 27 (2003).
40. J. R. Fienup, *Opt. Eng.* **19,** 297 (1980).
41. J. Miao et al., *Nature* **400,** 342 (1999).
42. E. Lima et al., *J. de Physique IV* **104,** 631 (2003).
43. V. Elser, *J. Opt. Soc. Am. A* **20,** 40 (2003).
44. T. O. Mentes et al., *J. Synch. Rad.* **9,** 90 (2002).
45. K. Green, *Tech. Report No. BNL-50522* (Brookhaven National Laboratory, 1976); A. M. Kondratenko, A. N. Skrinsky, *Opt. Spectr.* **42,** 189 (1977); S. Krinsky, *IEEE Trans. Nucl. Sci.* **NS-30,** 3078 (1983).
46. *X-ray Microscopy: Proceedings of the Sixth International Conference,* W. Meyer-Ilse et al., eds. (American Institute of Physics, Melville, NY, 2000), vol. 507.